

الموصلية طويلة الأجل من كسور ضيقة مليئة أحادي الطبقة بروبان في خزانات الغاز الصخري

ليو يوكسوان^{***}، جيانتشون جيو^{*}، جيا إكسينفينج^{**}، يوينج دوان^{*}، جيان ما^{*} وجينهونج هو^{*}
^{*} المختبر الرئيسي للنفط والغاز وخزان الجيولوجيا والاستغلال، جامعة البترول، وجنوب غرب تشنغدو 610500، الصين
^{**} إدارة المواد الكيميائية وهندسة البترول، كلية Schulich للهندسة، جامعة كالغاري، كالغاري، كندا

الخلاصة

الهدف الأساسي من التكسير الهيدروليكي هو إنشاء مسار عالي التوصيلية. يتم تكسير غاز الصخر الزيتي بشكل رئيسي بواسطة بقع الماء. يتم إنشاء شبكة معقدة من الكسور الثانوية الضيقة في تكسيرات بقع الماء. هذه الكسور الضيقة من دون بروبان تحافظ على خاصية توصيلية منخفضة. يمكن استخدام طبقة أحادية جزئية من البروبان لتعزيز التوصيلية لهذه الكسور ومن ثم تحسين الإنتاج. بسبب التفاعل بين البروبان وسطح الكسر تحت الضغط المحيط، يتم ترسيخ البروبان في التشكيلات، مما يؤدي إلى انخفاض عرض الكسر وفعالية التوصيل. الأبحاث المتاحة قد عالجت المشكلة. ومع ذلك، فإن الصخر الزيتي يكشف كميات متفاوتة من تشوهات التسرب في الاستجابة للضغوط التطبيقية، التي من شأنها أن تعزز باستمرار غرز البروبان وتخفيض عرض الكسور. تأثير هذا العامل الذي يعتمد على الوقت على التوصيلية على المدى الطويل للبروبان أحادي الطبقة الجزئي ليست مفهومة جيدا. يمكن الاستفادة من دراسة الخصائص والعوامل المسيطرة على التغيير على المدى الطويل في التوصيل لتحليل الإنتاج وتحسين التكسير الهيدروليكي. في هذه الدراسة يتم تطوير نماذج مدمجة في الطرق العددية والتحليلية لذلك. تم تطوير نموذج العنصر المحدود لمحاكاة التغيير على المدى الطويل في عرض الكسور. بعدها تم استخدام نموذج مبسط مبني على معادلة Garman-Kozeny لحساب الخاصية التوصيلية على المدى الطويل. وتشير نتائج المحاكاة أنه بعد النظر في آثار الزحف على المدى الطويل، لا يزال يوجد هناك تركيز من البروبان الأمثل، والذي لا يزال التوصيل الأقصى للبقايا بعد غرز البروبان. كما تشير نتائج المحاكاة أيضا إلى أن التركيز الأمثل يعتمد على الضغط والخصائص الميكانيكية للصخور والخصائص الميكانيكية للبروبان والوقت.

Long Term Conductivity of Narrow Fractures Filled with a Proppant Monolayer in Shale Gas Reservoirs

Yuxuan Liu ^{***}, Jianchun Guo^{*}, Xinfeng Jia^{**}, Youjing Duan^{*}, Jian Ma^{*} and Jinghong Hu^{*}

^{*} State Key Laboratory of Oil and Gas Reservoir Geology and Exploitation, Southwest Petroleum University, Chengdu 610500, China

^{**} Department of Chemical and Petroleum Engineering, Schulich School of Engineering, University of Calgary, Calgary T2N 1N4, Canada

^{***} Corresponding author: liuyx_6@163.com (Y.X. Liu)

ABSTRACT

The primary goal of hydraulic fracturing is to create a high conductive pathway. Gas shale is mainly fractured by slick-water. A complex network of narrow secondary fractures is created in slick water fracturing. These narrow fractures without proppants maintain low conductivity. A partial monolayer of proppant can be used to enhance the conductivity of these fractures and then improve the production. Due to the interaction between proppants and fracture surface under confining stress, the proppants will embed into the formations, which results in a decrease in fracture width and conductivity. Researches available in literature have addressed the problem. However, the shale reveals varying amounts of creep deformation in response to applied stress, which will continuously enhance the proppant embedment and reduce fracture width. The influence of this time dependent effect on the long term conductivity of partial monolayer proppant is not well understood. The study of the characteristics and controlling factors of the long term change in conductivity can benefit to the production analysis and hydraulic fracturing optimization. Therefore, models combining numerical and analytical methods are developed in this paper. A finite element model is developed to simulate the long term change in fracture width. Then a simplified model based on Carman-Kozeny equation is used to calculate the long term conductivity. Simulation results show that after considering long term creep effects, there is still an optimal proppant concentration, which remains the maximum residual conductivity after proppant embedment. The simulation results also indicate that the optimal concentration depends on stress, rock mechanical properties, proppant mechanical properties and time.

Keywords: Finite element method; fracture conductivity; hydraulic fracturing; proppant embedment; shale gas reservoirs.

INTRODUCTION

Shale gas is becoming an important energy source worldwide. The increasing significance of shale gas has led to the need for deeper understanding of shale behavior. Development of shale gas resources relies on drilling horizontal wells and massive multi-stage hydraulic fracturing, which is capital intensive. Deeper understanding of hydraulic fracturing can benefit the economic aspects of shale gas exploitation.

The hydraulic fracturing involves injecting a fluid at a pressure sufficiently high to break down the rock. To prevent the closure of hydraulic fracture after the treatment, a propping agent

is transported into the fracture to keep the fracture open and maintain a conductive flow path for the hydrocarbon production (Economides & Nolte, 2000). Therefore, the primary goal of hydraulic fracturing is to create a high conductive pathway (Cipolla, 2009). The flow capacity of the conductive path is reflected as fracture conductivity, which is the product of fracture width and permeability.

The fracture conductivity is typically maintained by filling the fracture with multiple layers of proppants, named as proppant packs as shown in Figure 1. However, a complex network of narrow secondary fractures, rather than bi-wing fractures, is created in gas shale by slick water fracturing. These fractures without proppants cannot maintain a relative high conductivity. A partial monolayer of proppant can be used to enhance the conductivity and then improve the production (Fredd et al., 2001). Therefore, the study of the conductivity of narrow fractures filled with a proppant monolayer can benefit the production analysis and optimization of hydraulic fracturing in gas shale.

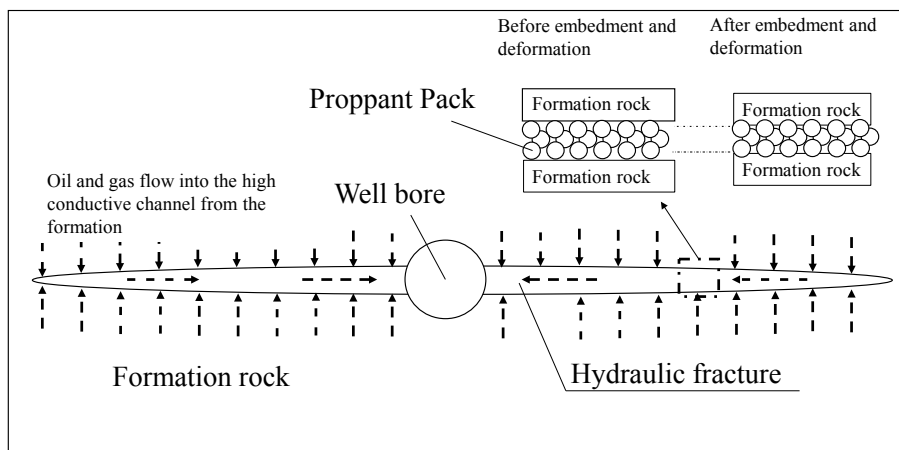


Fig. 1. Illustration of propped hydraulic fracture

Different mechanisms can contribute to the impairment of fracture conductivity including proppant embedment, non-Darcy flow, multi-phase flow, etc (Palisch et al., 2007). The relative contribution of each of the impairment mechanisms varies from one formation to the other, depending upon numerous variables including mechanical properties, mineral content, temperature, proppant type, fracture fluid type and closure pressure (Alramahi & Sundberg, 2012). The proppant embedment in soft formations with rich clay may enormously impair the fracture conductivity due to the decrease of fracture width up to 60% (Lacy et al., 1998). Proppant embedment is the direct result of rock deformation at the fracture face, when it is indented by the proppant with a loading perpendicular to fracture face imposed by the effective horizontal stress. (Alramahi & Sundberg, 2012)

Many scholars conducted laboratory studies on proppant embedment. (Huitt & McGlothlin Jr, 1958; Volk et al., 1981; Hartley & Bosma, 1985; Lacy et al., 1997; Lacy et al., 1998; Wen et al., 2007; Guo et al., 2008; Lu et al., 2008; Zhang et al., 2015). Experiment apparatus and methods have been developed. The effects of elastic modulus, closure pressure, water saturation, particle

size and distribution, proppant concentration, fluid viscosity and leakoff rate were investigated. In recent years, theoretical studies on modeling of proppant embedment have also been reported (Guo & Liu, 2012; Khanna et al., 2012; Neto & Kotousov, 2013; Li et al., 2014; Deng et al., 2014; Yan et al., 2016). However, these studies focused on the elastic deformation of rock. Elastic deformation only reflect the instantaneously behavior of shale. However, the shale is weak, unconsolidated and very fine-grained (average grain size less than 10 μm), with a composition of more than 50% clay, 30% quartz, and some minor amount of feldspar and plagioclase (Losh et al., 1999). The shale exhibits pronounced viscous creep behavior. The amount of shale volumetric creep strain for the same time period under the same pressure condition is 4 times larger than that of sand. (Chang & Zoback, 2009). The characteristics and controlling factors of long term conductivity due to creep is important in the analysis of production behavior and optimization of fracturing design. It is worthwhile to study the characteristic and controlling factors of long term change in conductivity of narrow fractures filled with proppant monolayer.

Therefore, models combining numerical and analytical methods are developed in this paper. In the present work, a finite element method (FEM) is used to model fracture width change due to proppant embedment. The model considers the simultaneous elastic and creep deformation of rock. Then a simplified model based on Carman-Kozeny equation is used to calculate the long term conductivity. Characteristics and controlling factors of narrow fracture conductivity are simulated.

THE NUMERICAL MODEL

Theoretical background

The deformation of shale shows a viscoelastic characteristic, which is the property of material that displays both viscous and elastic response, when subjected to load (Almasoodi, et al., 2014). Viscoelasticity can be visualized by two distinct phenomena, which are creep deformation and stress relaxation. The latter is outside of the scope of this paper. Creep deformation means that the shale exhibits a continuous increase in strain with time, when subjected to constant load.

A viscoelastic shale has an elastic deformation and a viscous deformation. The elastic deformation of shale is most commonly described by the stress-strain relationship of Hooke's Law. When rock is continuously subjected to high levels of stress, time dependent strain occurs. This time-dependent deformation is known as creep, which is the tendency of a solid material to move slowly or deform permanently under the influence of mechanical stresses. The rate of deformation is a function of rock properties, exposure time, temperature and the applied stress.

Sone & Zoback (2014) conducted laboratory tests on time dependent viscous deformation of shale gas reservoir rock. Results indicated that the time dependent deformation is an inherent property of the dry rock. This behavior can be described by a power law function of time, as follows:

$$\varepsilon = \sigma B t^n \quad (1)$$

where ε is the creep strain; σ is the applied stress, Pa; t is time, s; B and n are constant.

Mechanical induced change of fracture width and conductivity after fracturing involves two processes, proppant embedment and proppant deformation. The proppant embedment process includes the indentation of proppant into the rock and deformation of the rock (Li et al., 2014). The deformation of shale can be described by Equation . The proppant can be assumed as elastic body. Its deformation is also described by Hooke's Law. Contact mechanics can be used to solve the indentation of proppants into a body (Khanna et al., 2012).

The contact problem can be formulated as a constrained minimization problem, where the objective function to be minimized is the total potential energy $\Pi(u)$ of the bodies in contact. The energy for this system can be written as

$$\Pi(u) = \frac{1}{2}ku^2 - fu \quad (2)$$

where, k is stiffness matrix, u is the displacement field, and f is the external force. Several constrained minimization algorithms can be used to solve the problem of Equation , such as the penalty method, the lagrange multipliers method and the augmented lagrangian method. The results presented in this paper are based on the augmented lagrangian method according to the ANSYS implementation. The detailed analytical and numerical method on this problem can be found in reference (Johnson, 1987; Wriggers, 2006).

It should be noted that some simplifications were adopted in order to model the process, such as disregard of the secondary cracking of the fracture wall and crushing of proppants. The elastic and creep deformation is considered to be the primary mechanism of fracture conductivity loss.

Model implementation

A narrow fracture filled with partial monolayer proppants is subjected to confining stress. In hydraulic fracturing, the confining stress is also called closure pressure. The width of the fracture diminishes due to the compaction of proppants and embedment of proppants into fracture face. Due to the strong nonlinearity of contact problem, the numerical model was implemented in the finite element code ANSYS static structural code. A physical model for embedment is shown in Figure 2. The boundary conditions of the model are the same to that in the experimental tests (Lacy et al., 1997; Lacy et al., 1998; Fredd et al., 2001; Wen et al., 2007). The rock length is L , fracture width is w_f , rock width is w_r and proppant radius is r . A confining stress is applied on the top of the rock, while the bottom of the rock is fixed. The sides of the rock are fixed to x movement. FEM requires meshing the system to be analyzed into a finite number of elements. In ANSYS software, the mesh profile can be generated manually or automatically by a special algorithm in the software. In this simulation, a face mesh with refinement is used.

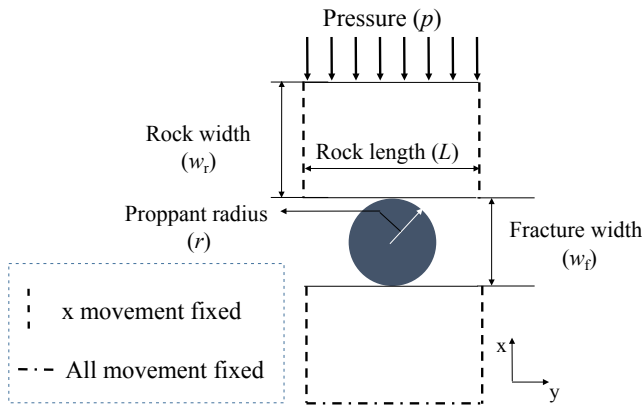


Fig. 2. illustration of calculation domain and boundary conditions

In order to reflect the features of the sparse distribution of proppants, a normalized parameter called distance ratio (P_{dr}), is introduced as illustrated in Figure 3, which is

$$P_{dr} = \frac{4r}{L} \tag{3}$$

where L is rock length, m; r is particle radius, m. If the two packs are close to each other, the P_{dr} is equal to unity; if not, P_{dr} is smaller than unity. The parameter is also a reflection of proppant concentration in the narrow fracture.

According to the relationship between the pressure difference in section 1 and section 2, the equivalent permeability of section 1 and section 2 is

$$\frac{1}{k_{eq}} = \frac{1}{k_1} (1 - P_{dr}) + \frac{1}{k_2} P_{dr} \tag{4}$$

where k_1 is the permeability of the void space without proppant (section 1), m^2 ; k_2 is the permeability of proppant pack (section 2), m^2 ; k_{eq} is the equivalent permeability of section 1 and section 2, m^2 .

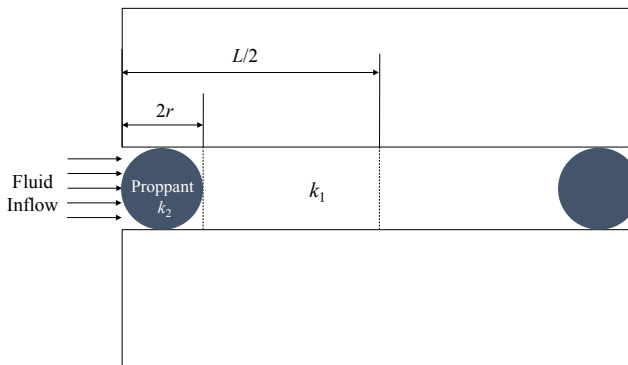


Fig. 3. Illustration of conductivity calculation

The conductivity of section 1 is

$$k_1 = \frac{w_f^2}{12} \tag{5}$$

The Carman-Kozeny model is used to calculate the permeability of the proppant packs (section 2) as follows (Kaviany, 1995):

$$k_2 = \frac{\phi^3}{180(1-\phi)^2} d^2 \tag{6}$$

where, w_f is fracture width, m; ϕ is the porosity of the sample; d is sphere diameter, m. This equation has been validated in calculating permeability of proppant pack (Sanematsu et al., 2015).

Then the fracture conductivity can be obtained by

$$F_c = k_{eq} \times w_f \tag{7}$$

where, F_c is the fracture conductivity, m^2 . The residual conductivity after proppant embedment and deformation is normalized against the conductivity of fracture with a width equals to the initial width ($2r$), marked as F_{cn} .

DISCUSSION

Model verification

To verify the FEM model, it is necessary to compare the FEM model with the existing models. Li et al. (2014) developed a model to calculate proppant embedment with consideration of the elastic process. With the basic data in Table 1, the results of the two models are illustrated in Figure 4. The values calculated with the FEM model and the model of (Li et al., 2014) overlap each other. This verifies the effectiveness of the FEM model for the elastic deformation and contact calculation. For the width change with time, Figure 5 shows the comparison between analytical results and FEM model. The analytical results are calculated based on models of Li et al. (2014) and Sone & Zoback (2014) using the basic data in Table 1. The two results are close to each other with a maximum error less than 5%. This verifies the effectiveness of the FEM model for the creep deformation. Therefore, it is reasonable to use the FEM model.

Table 1. Basic parameters

| Poisson's ratio of proppant | Poisson's ratio of rock | Young's modulus of proppant (MPa) | Young's modulus of rock (MPa) | Radius of proppant (mm) | Thickness of rock (mm) | n |
|-----------------------------|-------------------------|-----------------------------------|-------------------------------|-------------------------|------------------------|-------|
| 0.13 | 0.13 | 21306 | 20000 | 0.325 | 20 | 0.062 |

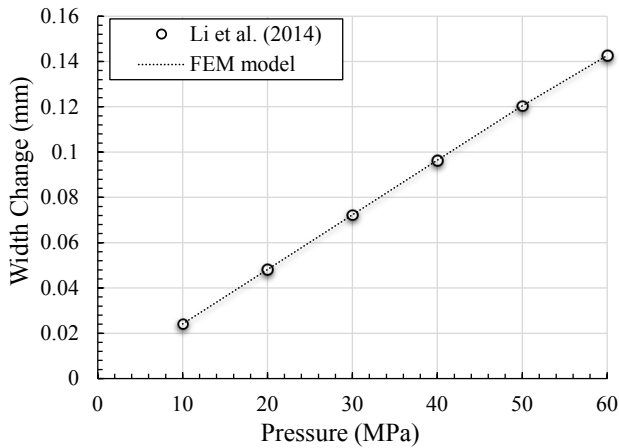


Fig. 4. Comparison of width change predicted by the two models

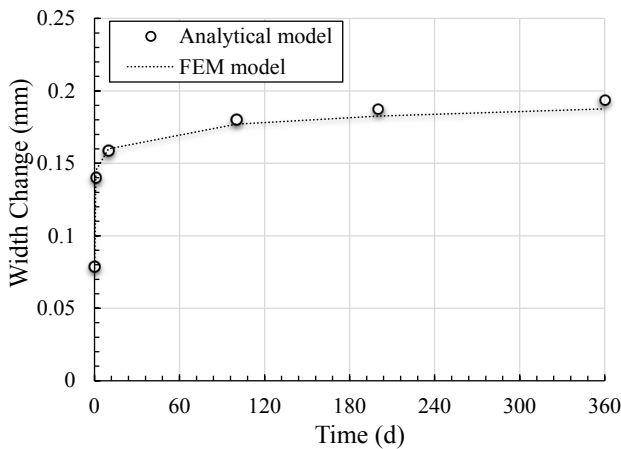
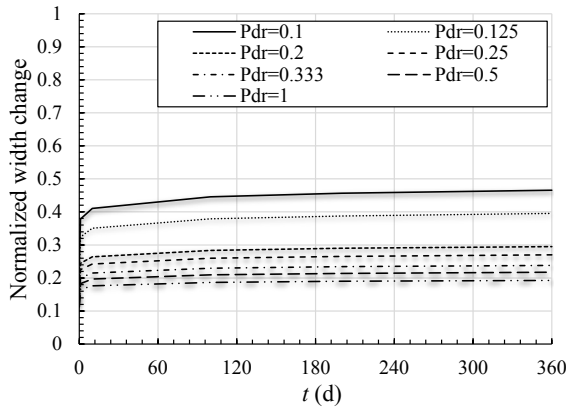


Fig. 5. Comparison of width change with time

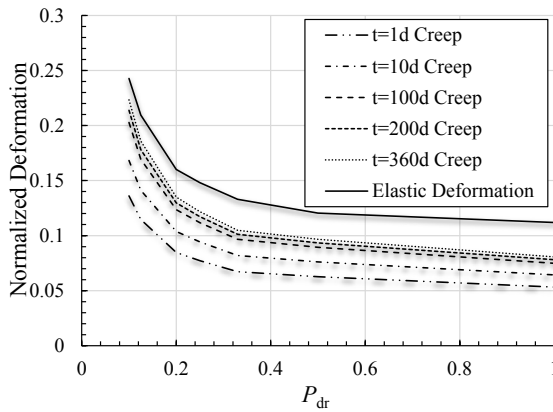
Characteristics of long term conductivity

The fracture width change and deformation of different mechanisms are normalized against a width equals to the initial width ($2r$). If not otherwise specified, the confining stress is 30MPa. Figure 6 illustrates the fracture width change with time at different P_{dr} . As shown in the figure, the change in fracture width increases with time, resulting in a continuous decrease in fracture width. With a decrease in P_{dr} , the long term effect is more obvious. This is because, with a decrease in P_{dr} , less proppants remain in the fracture to support its opening. The force acting on the single particle is larger and long term creep is more obvious. However, after 100d, the change in the fracture width is relatively small for different P_{dr} . This indicates that the decrease of fracture width mainly happens in the initial production stages. The instantaneous elastic deformation dominates the change of fracture width under the simulated conditions (Figure 6b). However, at $P_{dr} = 0.1$

and time = 360d, the creep deformation is close to the elastic deformation. When the proppant concentration is small, with the increase of production time, the width reduction caused by creep deformation may exceed the elastic deformation, thus becoming the main factors affecting the width change.



(a) Fracture width change with time at different Pdr



(b) Comparison between different mechanisms

Fig. 6. Change in fracture width with time at different Pdr

Long term fracture conductivity can be obtained with the known conditions, $n=0.062$ and $B=5 \times 10^{-5} \text{MPa}^{-1}$, as shown in Figure 7. The initial conductivity decreases with P_{dr} , because more proppants occupy the void space, resulting in decreased permeability. The change in residual conductivity after proppant embedding is more complex. With an increase in P_{dr} , the fracture conductivity first increases to a certain value and then decreases. In other words, there is an optimal P_{dr} , which has the maximum conductivity after proppant embedment and deformation. This is because with an increase in P_{dr} , there are two different effects on conductivity: (1) a reduction in proppant deformation and embedment due to more proppants supporting the confining stress, which decreases the loss of conductivity and (2) an increase in the loss of

conductivity due to a reduced void volume, which is occupied by more proppants. The curve trend is the same as the calculations done by Khanna et al. (2012), in which the conductivity is computed by Ansys CFX.

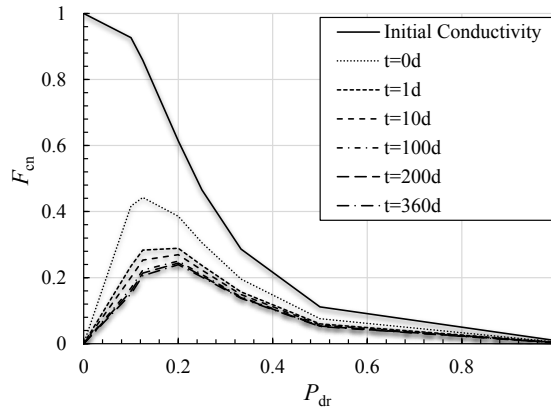


Fig. 7. Relationship between initial conductivity and conductivity after embedding

Influencing factors of long term conductivity

From Equation , the long term conductivity is determined by two important parameters: the stress and parameter B. According to Sone & Zoback (2014), the parameter B essentially reflects the instantaneous elastic modulus of the rock. The elastic modulus of rock (E) nearly equals to $1/B$. Then a normalized parameter can be defined as follows:

$$P_n = \frac{\sigma}{E} \quad (8)$$

where E is the Young's modulus of rock, Pa. From Equation , the new normalized parameter reflects the influence of B and stress simultaneously.

Figure 8 shows the relationship between proppant distance ratio (P_{dr}) and normalized conductivity (F_{cn}) at different normalized stress (P_n) for four different times. The results demonstrate that for any pressure and time conditions, there exists an optimal proppant distance or concentration, which has the maximum conductivity after proppant embedment. At high confining stress or low rock elastic modulus, the optimal proppant distance is high, which means that the proppant should be placed closer to each other. At low pressure or high rock elastic modulus, the proppant can be placed more diffuse. Besides, at lower confining stress ($P_n=0.00075$ and $P_{dr}=0.0015$) the optimal distance has no obvious change from 1d to 360d. At higher pressure ($P_{dr}=0.003$), the optimal distance shows a slightly change. This trend indicates that with an increase in stress or a decrease in rock elastic modulus, the effect of creep on the optimal concentration will be more obvious.

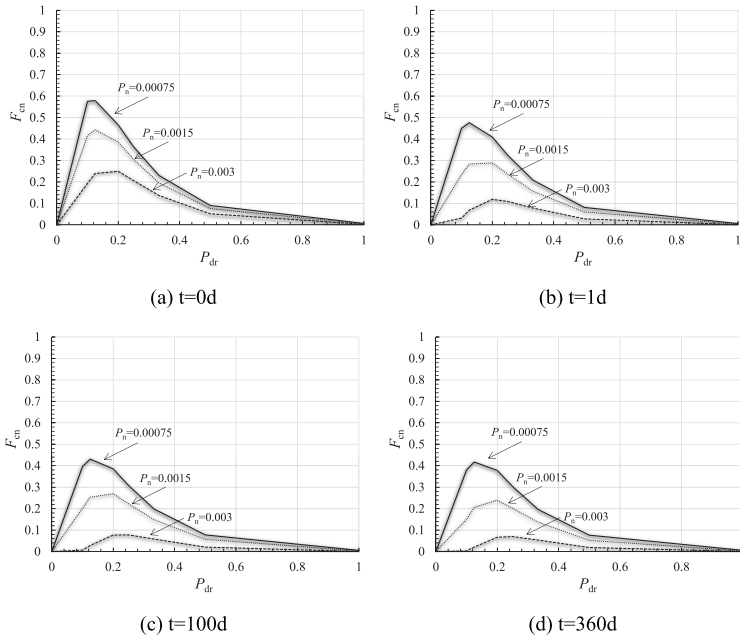


Fig. 8. Effect of pressure and rock elastic modulus on conductivity

Figure 9 shows the comparison between elastic and creep deformation for three different times in Figure 8. As can be seen in the figure, with an increase in time and stress, the elastic and creep deformation increase as expected. Under high confining stress or low rock elastic modulus, the creep deformation will be the dominant factors controlling the closing of fracture (Figure 9c).

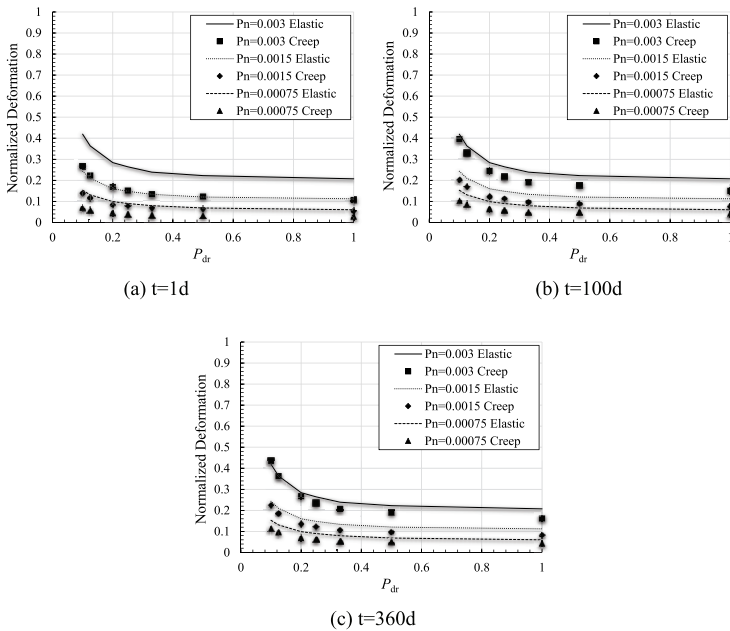


Fig. 9. Comparison between elastic and creep deformation

CONCLUSIONS

In this paper, the characteristic and controlling factors of partial monolayer proppant were studied. The following conclusions can be drawn according to the present study:

- (1) Calculation in this manuscript demonstrates that long term effects should be considered in the determination of proppant concentration. After considering the long term creep deformation, there is still an optimal proppant concentration, which has the maximum conductivity after considering proppant embedment. Besides, the calculated optimal proppant concentration becomes larger than that without considering long term effect.
- (2) The optimal proppant concentration depends on stress, rock mechanical properties, proppant mechanical properties and time. With an increase in closure pressure or a decrease in rock elastic modulus, the proppant should be placed closer to each other.

ACKNOWLEDGEMENTS

The authors would like to thank the financial support of National Natural Science Foundation of China (No.51374178), the Young scholars development fund of SWPU (201599010084), and PLN1301 of State Key Laboratory of Oil and Gas Reservoir Geology and Exploitation (Southwest Petroleum University), National Science and Technology Major Project (No. 2016ZX05002-002).

NOMENCLATURE

B - Constant

d - Sphere diameter, m

E - Young's modulus of rock, Pa

f - External force.

F_c - Fracture conductivity, m.m²

F_{cn} - Normalized conductivity, dimensionless

k - Stiffness matrix

k_1 - Permeability of the void space without proppant(section 1), m²

k_2 - Permeability of proppant pack(section 2), m²

k_{eq} - Equivalent permeability of section 1 and section 2, m².

L - Rock length, m

n - Constant

P_{dr} - Proppant distance ratio, dimensionless

P_n - Normalized stress, dimensionless

r - Particle radius, m

t - Time, s

u - Displacement field

w_f - Fracture width, m;

ε is the creep strain

σ - Applied stress, Pa

ϕ - Porosity of the sample, dimensionless

REFERENCES

- Alramahi, B. & Sundberg, M.I. 2012.** Proppant embedment and conductivity of hydraulic fractures in shales. Paper ARMA-2012-291, presented at 46th US Rock Mechanics/Geomechanics Symposium, Chicago, Illinois.
- Almasoodi, M.M., Abousleiman, Y.N. & Hoang, S.K. 2014.** Viscoelastic Creep of eagle ford shale: investigating fluid-shale interaction. Paper SPE171569, presented at SPE/CSUR Unconventional Resources Conference, Calgary, Alberta, Canada.
- Cipolla, C. 2009.** Modeling production and evaluating fracture performance in unconventional gas reservoirs, *Journal of Petroleum Technology*, **61** (9): 84-90.
- Chang, C. & Zoback, M.D. 2009.** Viscous creep in room-dried unconsolidated Gulf of Mexico shale (I): Experimental results. *Journal of Petroleum Science and Engineering*, **69**(3): 239-246.
- Deng, S.C., Li, H.B., Ma, G.W., Huang, H. & Li, X. 2014.** Simulation of shale–proppant interaction in hydraulic fracturing by the discrete element method, *International Journal of Rock Mechanics and Mining Sciences*, **70**: 219-228.
- Economides, M.J. & Nolte, K.G. 2000.** Reservoir stimulation (3rd Ed). Wiley, England.
- Fredd, C.N., McConnell, S.B., Boney, C.L. & England K.W. 2001.** Experimental study of fracture conductivity for water-fracturing and conventional fracturing applications. *SPE Journal*, **6**(3): 288-298.
- Guo, J.C., Lu, C., Zhao, J.Z. & Wang, W.Y. 2008.** Experimental Research on Proppant Embedment. *Journal of China Coal Society*, **33**(6): 661-664. (In Chinese)
- Guo, J.C. & Liu, Y.X. 2012.** Modeling of proppant embedment: elastic deformation and creep deformation, Paper SPE 157449, presented at SPE international Production and Operations Conference & Exhibition, Doha, Qatar.
- Huitt, J.L. & McGlothlin Jr, B.B. 1958.** The Propping of fractures in formations susceptible to propping-sand embedment, Paper SPE 58-115, presented at the spring meeting of the Pacific Coast District, Division of Production, Los Angeles, Calif, U.S.A
- Hartley, R. & Bosma, M. 1985.** Fracturing in chalk completions (includes associated papers 14483 and 14682). *Journal of Petroleum Technology*, **37**(1):73-79
- Johnson, K.L. 1987.** Contact mechanics. Cambridge University Press Cambridge.
- Khanna, A., Kotousov, A., Sobey, J. & Weller, P. 2012.** Conductivity of narrow fractures filled with a proppant monolayer. *Journal of Petroleum Science and Engineering*, **100**: 9-13.
- Kaviany, M. 1995.** Principles of heat transfer in porous media (2nd Ed). Springer, Berlin.
- Lacy, L.L., Rickards, A.R. & Ali, S.A. 1997.** Embedment and fracture conductivity in soft formations associated with HEC, Borate and water-based fracture designs. Paper SPE 38590, presented at the SPE Annual technical Conference and exhibition, San Antonio, Texas, U.S.A
- Lacy, L.L., Rickards, A.R. & Bilden, D.M. 1998.** Fracture width and embedment testing in soft reservoir sandstone. *SPE Drilling & Completion*, **13**(1): 25-29
- Lu, C., Guo, J.C., Wang, W.Y., Deng, Y. & Liu D.F. 2008.** Experimental research on proppant embedment and its damage to fractures conductivity. *Natural Gas Industry*, **28**(2): 99-101 (In Chinese).
- Li, K.W., Gao, Y.P., Lv, Y.C. & Wang, M. 2014.** New mathematical models for calculating proppant embedment and fracture conductivity. *SPE Journal*, **20**(3): 496 - 507

- Losh, S., Eglinton, L., Schoell, M. & Wood, J. 1999.** Vertical and lateral fluid flow related to a large growth fault, South Eugene Island Block 330 Field, offshore Louisiana. *AAPG bulletin*, **83**(2): 244-276.
- Neto, L.B. & Kotousov, A. 2013.** Residual opening of hydraulic fractures filled with compressible proppant. *International Journal of Rock Mechanics and Mining Sciences*, **61**: 223-230.
- Palisch, T.T., Duencel, R.J., Bazan, L.W., Heidt, H.J. & Turk G.A. 2007.** Determining realistic fracture conductivity and understanding its impact on well performance-theory and field examples, Paper SPE 106301, presented at the SPE Hydraulic Fracturing Technology Conference, College Station, Texas, U.S.A.
- Sone, H., & Zoback, M. D. 2014.** Time-dependent deformation of shale gas reservoir rocks and its long-term effect on the in situ state of stress. *International Journal of Rock Mechanics and Mining Sciences*, **69**: 120-132.
- Sanematsu, P., Shen, Y., Thompson, K., Yu, T., Wang, Y., Chang, D. L. & Willson, C. 2015.** Image-based Stokes flow modeling in bulk proppant packs and propped fractures under high loading stresses. *Journal of Petroleum Science and Engineering*, **135**: 391-402.
- Volk, L.J., Raible, C.J., Carroll, H.B. & Spears, J.S. 1981.** Embedment of high strength proppant into low-permeability reservoir rock, Paper SPE/DOE 9867, presented at the 1981 SPE/DOE Low Permeability Symposium, Denver, Colorado, U.S.A
- Wen, Q.Z., Zhang, S.C., Wang, L., Liu, Y.S. & Li, X.P. 2007.** The effect of proppant embedment upon the long-term conductivity of fractures. *Journal of Petroleum Science and Engineering*, **55**(3): 221-227
- Wriggers, P. 2006.** *Computational contact mechanics*(2nd Ed). Springer, Berlin.
- Yan, X., Huang, Z., Yao, J., Song, W., Li, Y. & Gong, L. 2016.** Theoretical analysis of fracture conductivity created by the channel fracturing technique. *Journal of Natural Gas Science and Engineering*, **31**:320-330.
- Zhang, J.J., Ouyang, L.C., Zhu, D. & Hill, A.D. 2015.** Experimental and numerical studies of reduced fracture conductivity due to proppant embedment in the shale reservoir. *Journal of Petroleum Science and Engineering*, **130**:37-45.

Submitted: 1/June/2016

Revised : 26/July/2016

Accepted : 28/July/2016